

J. Electroanal. Chem., 318 (1991) 379–386
Elsevier Sequoia S.A., Lausanne
JEC 01869

Preliminary note

Surface phase transition of ordered iodine monolayers on a Pt(111) electrode as studied by normal incidence optical second harmonic generation

Matthew L. Lynch and Robert M. Corn *

Department of Chemistry, University of Wisconsin, 1101 University Ave., Madison, WI 53706 (USA)

(Received 30 September 1991; in revised form 8 October 1991)

The spectroscopic study of electrochemical surfaces provides the modern electrochemist with the detailed information required for the interpretation of charge transfer processes at solution/electrode interfaces. Fundamental surface reactions such as catalytic oxidation and thin film growth can depend critically upon the local adsorbate structure at the electrode surface. This adsorbate structure will vary with changes in the morphology of the substrate, the concentrations of solution phase species, and the electrostatic fields at the surface. Through a combination of in situ and ex situ spectroscopic measurements, a detailed molecular level understanding of the important adsorbate–surface interactions can be obtained [1].

Optical second harmonic generation (SHG) is a surface-selective spectroscopic technique that has been applied to the in situ study of a variety of metal electrode surfaces [2–4]. In a surface SHG experiment, changes in the electronic surface structure of an electrode upon adsorption are correlated with changes in the elements of the surface nonlinear susceptibility tensor χ as measured by the potential and polarization dependence of the SHG signal [5]. At single crystal surfaces, additional tensor elements of χ may appear due to a reduction in surface symmetry upon adsorption or surface reconstruction [6–8]. In a series of recent papers [9] we have reported the use of SHG at well-ordered Pt(111) electrodes. A reduction in the surface symmetry was observed in the presence of adsorbed monolayers of iodine, CO and hydrogen on the platinum surface. In this note we demonstrate how SHG measurements performed at an incident angle of 0° (normal incidence) can further elucidate the reduction of surface symmetry upon

* To whom correspondence should be addressed.

adsorption at the Pt(111) interface. In particular, the surface phase transition between two ordered iodine monolayers on a Pt(111) electrode is monitored by normal incidence SHG measurements of the average electrode surface symmetry as a function of potential.

A Pt(111) crystal (Aremco) was prepared by annealing in a hydrogen flame and subsequent exposure to an argon-iodine vapor atmosphere [10–12]. This procedure has been found to produce a well-ordered Pt(111) surface with a $(\sqrt{7} \times \sqrt{7})R19.1^\circ$ iodine monolayer [11–13]. The crystal was then placed in a 0.1 mM potassium iodide (Aldrich) solution that was adjusted to a pH of 4 by addition of dilute perchloric acid (GFS Chemicals) and to a supporting electrolyte concentration of 10 mM with sodium fluoride (Fluka). Light at 605 nm was focused onto the electrode to within two degrees of the surface normal, and the reflected second harmonic intensity was detected with photon counting techniques [5,9]. The normal incidence SHG signal from the Pt(111) crystal was obtained by rotation of the input polarization from 0° to 360° while measuring the second harmonic light with an output polarization parallel to either the x or y crystal axes, where x and y are defined as the $[2 - 1 - 1]$ and $[01 - 1]$ crystal directions respectively. The SHG polarization anisotropy obtained at a potential of 0.050 V vs. a sodium chloride-saturated calomel electrode (SSCE) is shown in Fig. 1. Ex situ LEED emersion experiments have shown that at this potential the $(\sqrt{7} \times \sqrt{7})$ iodine monolayer is present on the surface [13]. The intensity of the SHG signal polarized along the y crystal axis direction, $I_y(2\omega)$, is four-fold symmetric, whereas the SHG signal polarized along the x crystal axis direction, $I_x(2\omega)$, shows four peaks of alternating intensity. To facilitate the analysis, the polarization anisotropies are also displayed in polar coordinates.

The anisotropy patterns in Fig. 1 can be explained in terms of the surface symmetry of the Pt(111) electrode. For (111) surfaces, the total surface symmetry is defined by the arrangement of the first three atomic layers [14]. In the absence of reconstruction, a Pt(111) electrode will have C_{3v} surface symmetry. Surfaces of this symmetry have four unique surface tensor elements: χ_{ZZZ} , χ_{ZXX} , χ_{XXZ} , and χ_{XXX} [15]. Selection of a normally incident geometry greatly simplifies the SHG response from a surface by the elimination of all surface tensor elements that contain the Z axis direction (the surface normal). For a C_{3v} surface, only χ_{XXX} will contribute to the normal incidence experiment*. The normal incidence polarization anisotropy from a C_{3v} surface will have the functional form [6,7,16]:

$$I_x(2\omega) \propto |\chi_{XXX}|^2 \cos^2(2\phi) \quad (1)$$

$$I_y(2\omega) \propto |\chi_{XXX}|^2 \sin^2(2\phi) \quad (2)$$

* Only surface contributions to the normal incidence SHG signal are considered in this paper. No higher order bulk contributions were observed in these SHG experiments; i.e., after electrochemical disordering of the surface, no SHG signal could be measured in the normal incidence experiment.

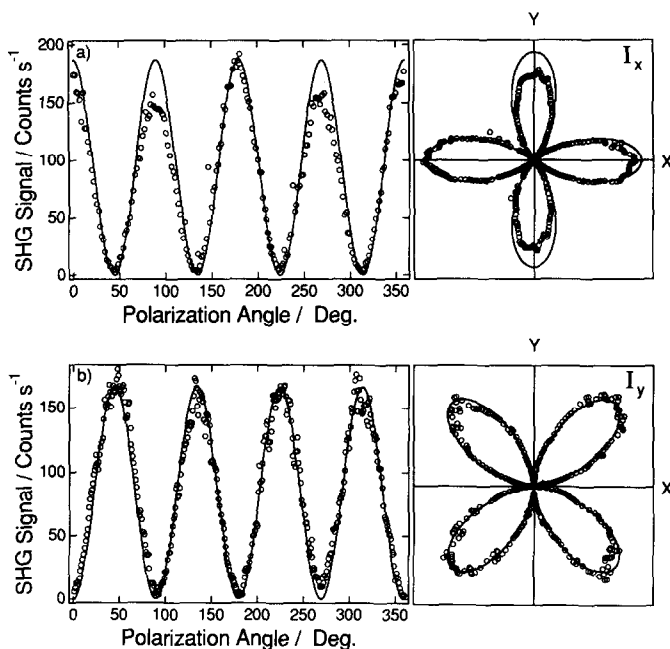


Fig. 1. Normal incidence polarization anisotropies $I_x(2\omega)$ and $I_y(2\omega)$ for the Pt(111) surface with a $(\sqrt{7} \times \sqrt{7})R19.1^\circ$ iodine monolayer at an electrode potential of 0.050 V. (a) x -polarized output, $I_x(2)$; (b) y -polarized output, $I_y(2\omega)$. The anisotropies are plotted both in linear coordinates, where the polarization angle ϕ is defined as the angle between the fundamental polarization vector and the x crystal axis direction, and in polar coordinates where the x and y crystal axes are labelled in the graph. The solid lines are theoretical curves for the normal incidence polarization anisotropies from a surface with C_{3V} symmetry.

where ϕ is defined as the angle between the x crystal axis and the plane of polarization. The functional forms of eqns. 1 and 2 lead to the symmetric four-fold patterns plotted as solid lines in Figs. 1a and 1b. As seen in Fig. 1a, the $I_x(2\omega)$ data do not fit the functional form for a C_{3V} surface. A reduction of the average surface symmetry from C_{3V} to C_{1V} is required to reproduce the alternating four-fold pattern observed for the polarization anisotropy. For a C_{1V} surface there are three independent tensor elements that can contribute to the normal incidence experiment: χ_{XXX} , χ_{XYX} , and χ_{YXY} [6], and the normal incidence polarization anisotropy takes on the functional form:

$$I_x(2\omega) \propto |\chi_{XXX} \cos^2(\phi) + \chi_{XYX} \sin^2(\phi)|^2 \quad (3)$$

$$I_y(2\omega) \propto |\chi_{YXY}|^2 \sin^2(2\phi) \quad (4)$$

For the C_{1V} surface, $I_y(2\omega)$ remains a four-fold symmetric pattern, and $I_x(2\omega)$ can display an alternating four-fold pattern depending upon the relative magnitude and phase of χ_{XXX} and χ_{XYX} . The data for $I_x(2\omega)$ shown in Fig. 1a can be fitted

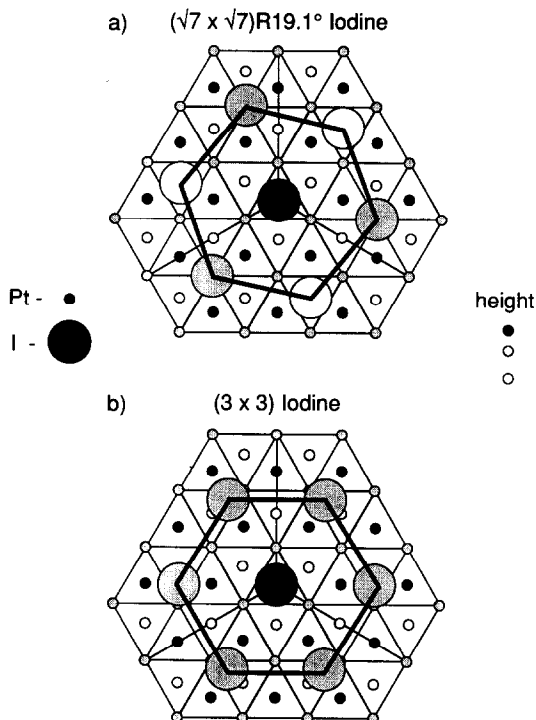


Fig. 2. Proposed iodine structures on a Pt(111) electrode: (a) the $(\sqrt{7} \times \sqrt{7})R19.1^\circ$ iodine monolayer, surface coverage = $3/7$ (0.429); (b) the (3×3) iodine monolayer, surface coverage = $4/9$ (0.444). The iodine atoms in the $(\sqrt{7} \times \sqrt{7})R19.1^\circ$ monolayer are situated either on an *a*-top site, a three-fold coordinate shallow hollow, or a three-fold coordinate deep hollow as indicated by the black, gray, white shading respectively. The iodine atoms in the (3×3) iodine monolayer are situated on either an *a*-top site or a two-fold coordinate bridging site as indicated by the black and gray shading respectively.

assuming a 180° phase shift between χ_{XXX} and χ_{XYX} and a ratio of $\chi_{XXX}/\chi_{XYX} = -1.1$. These normal incidence polarization anisotropy equations are described in greater detail elsewhere [16]; a similar reduction in symmetry has been determined by normal incidence SHG experiments at Si(111) surfaces [6].

The reduction of the average surface symmetry from C_{3V} to C_{1V} is an unexpected result for the $(\sqrt{7} \times \sqrt{7})$ iodine monolayer. A diagram of the $(\sqrt{7} \times \sqrt{7})R19.1^\circ$ iodine monolayer is shown in Fig. 2a. This structure has a surface coverage of three iodine atoms per seven platinum atoms ($\theta = 0.429$), and the overall surface symmetry should be reduced from C_{3V} to C_3 . In previous off-normal SHG rotational anisotropy experiments on Pt(111) electrodes with the $(\sqrt{7} \times \sqrt{7})$ iodine monolayer, the appearance of additional surface tensor elements were attributed to this reduction of surface symmetry [9]. For a surface with C_3 symmetry, there are two independent tensor elements that can contribute to the

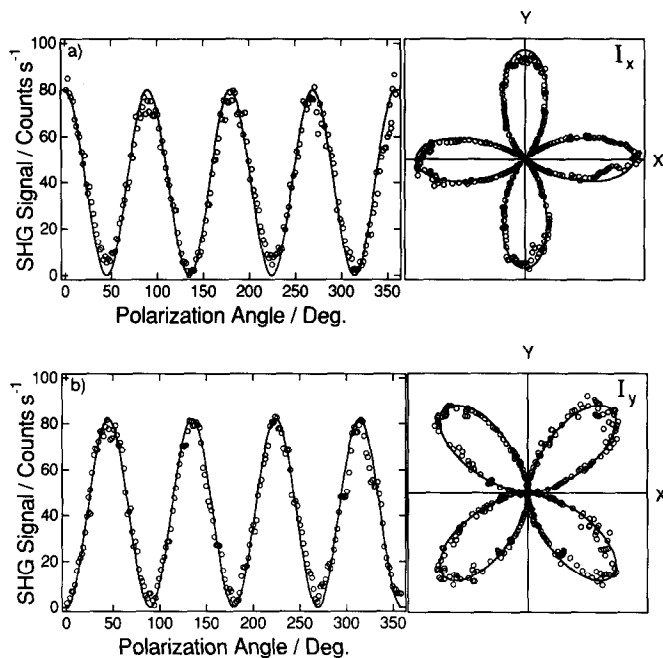


Fig. 3. Normal incidence polarization anisotropies $I_x(2\omega)$ and $I_y(2\omega)$ for the Pt(111) surface with a (3×3) iodine monolayer at an electrode potential of 0.550 V. (a) x -polarized output, $I_x(2\omega)$; (b) y -polarized output, $I_y(2\omega)$. The anisotropies are plotted in both linear and polar coordinates as defined in Fig. 2.

normal incidence experiment: χ_{XXX} and χ_{YYY} . The normal incidence polarization anisotropy would in this case take on the functional form:

$$I_x(2\omega) \propto |\chi_{XXX} \cos(2\phi) - \chi_{YYY} \sin(2\phi)|^2 \quad (5)$$

$$I_y(2\omega) \propto |\chi_{XXX} \sin(2\phi) + \chi_{YYY} \cos(2\phi)|^2 \quad (6)$$

In the normal incidence SHG experiments reported here we find that $\chi_{YYY} = 0$. However, the observation of a nonzero χ_{XYY} requires that the average surface symmetry be no higher than C_{1V} . This suggests that the adsorption of the $(\sqrt{7} \times \sqrt{7})$ iodine monolayer has forced the Pt(111) electrode to reconstruct in some manner that has lowered the overall surface symmetry. A similar reconstruction of a single crystal electrode has been observed at Au(111) surfaces with SHG [8c].

If the electrode potential is scanned to 0.550V, the $I_x(2\omega)$ and $I_y(2\omega)$ normal incidence anisotropy patterns change to the symmetric four-fold patterns shown in Fig. 3a and Fig. 3b, respectively. At this potential, ex situ LEED and in situ STM measurements have shown that the iodine monolayer has changed to the (3×3) overlayer pattern depicted in Fig. 2b. This overlayer structure has a surface coverage of four iodine atoms per nine platinum atoms ($\theta = 0.444$), which is slightly higher than that observed for the $(\sqrt{7} \times \sqrt{7})$ monolayer ($\theta = 0.429$). The

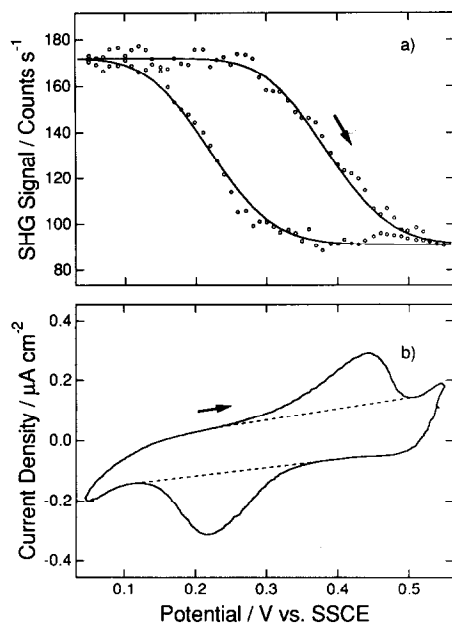


Fig. 4. (a) The potential dependence of the normal incidence SHG signal (x -polarized input, x -polarized output) during a CV which cycles between the two iodine monolayers (scan rate = 10 mV/s). (b) The cyclic voltammogram observed during the iodine phase transition. Integration of the current (indicated by the dotted lines) for the quasi-reversible peaks resulted in a change in surface charge density for the phase transition of $1.5 \mu\text{C}/\text{cm}^2$.

overall surface symmetry for the Pt(111) surface with the (3×3) iodine monolayer is C_{3V} , and the normal incidence SHG experiments confirm that in situ the electrode indeed maintains a C_{3V} surface symmetry (eqn. 1). Note the high sensitivity of the SHG experiment; even though the change in iodine surface coverage is only 0.016, the change in symmetry results in a large change in the SHG normal incidence polarization anisotropy.

Monitoring the normal incidence SHG signal while scanning the potential between 0.050 V and 0.550 V permits the real time observation of the phase transition between the two iodine monolayers. Figure 4a plots the normal incidence SHG signal (with both the input and output polarizations set along the x crystal axis) as a function of potential during a CV at a scan rate of 10 mV/s. A change in SHG signal level is clearly observed as the iodine switches back and forth from the $(\sqrt{7} \times \sqrt{7})$ to the (3×3) monolayers. Note the hysteresis in the SHG signal as the surface phase transition occurs; the amount of hysteresis depends on the scan rate. The average transition potential of ca. 0.300 V is close but not identical to the 0.190 V determined in the emersion experiments of Lu et al. [13b]. In addition to the SHG signal, the CV obtained from the iodine-coated Pt(111) electrode is shown in Fig. 4b. A very small quasi-reversible peak is

observed in the CV that coincides with the addition or removal of iodine atoms required to affect the surface phase transition:

$$I_{(aq)}^- \rightleftharpoons I_{ads} + e^- \quad (7)$$

Integration of the current in this peak yields a charge density of $1.5 \pm 0.5 \mu\text{C}/\text{cm}^2$. The theoretical charge density for an iodine phase transition with a change in surface coverage of $\Delta\theta = 0.016$ is $3.8 \mu\text{C}/\text{cm}^2$ *. The discrepancy between the theoretical and experimental values could be due to either capacitive charging effects, or to the slight surface reconstruction observed for the $(\sqrt{7} \times \sqrt{7})$ monolayer.

In summary, this paper describes the application of normal incidence SHG polarization anisotropy experiments to the measurement of the average surface symmetry of well-ordered Pt(111) electrodes. The phase transition from a $(\sqrt{7} \times \sqrt{7})R19.1^\circ$ iodine monolayer to a (3×3) monolayer is observed in real time with the SHG signal. Analysis of the normal incidence polarization anisotropy for the two monolayers leads to the conclusion that the (3×3) monolayer has an average surface symmetry of C_{3v} and the $(\sqrt{7} \times \sqrt{7})$ monolayer has an average surface symmetry of C_{1v} . This latter surface can only occur if there is some surface reconstruction of the monolayer and/or substrate in the electrochemical environment. These experiments demonstrate that the normal incidence SHG anisotropy experiment is a powerful method for the determination of average surface symmetry at single crystal electrodes.

ACKNOWLEDGMENT

The authors would like to acknowledge the support of the National Science Foundation for this research.

REFERENCES

- 1 (a) A.T. Hubbard, *Chem. Rev.*, 88 (1988) 633; (b) P.N. Ross and R.N. Wagner, in H. Gerischer (Ed.), *Advances in Electrochemistry and Electrochemical Engineering*, Vol. 13, Wiley, New York, 1984; (c) A. Bewick and S. Pons, in R.J.H. Clark and R.E. Hester (Eds.), *Advances in Infrared and Raman Spectroscopy*, Vol. 12, Wiley-Heyden, London, 1985; (d) R.K. Chang and T.E. Furtak, (Eds.), *Surface Enhanced Raman Scattering*, Plenum Press, New York, 1982.
- 2 R.M. Corn, *Anal. Chem.*, 63, (1991) 285A.
- 3 (a) G.L. Richmond, *Electroanal. Chem.*, (A.J. Bard, Ed.), 17 (1991) 87; (b) G.L. Richmond, *Prog. Surf. Sci.*, 28 (1988) 1.
- 4 (a) Y.R. Shen, *Annu. Rev. Phys. Chem.*, 40 (1989) 327 and references therein; (b) Y.R. Shen, *The Principles of Nonlinear Optics*, Wiley, New York, 1984.
- 5 D.J. Campbell, M.L. Lynch, and R.M. Corn, *Langmuir*, 6 (1990) 1656.
- 6 T.F. Heinz, M.M.T. Loy and W.A. Thompson, *Phys. Rev. Lett.*, 54 (1985) 63.
- 7 J. Miragliotta and T.E. Furtak, *Phys. Rev.*, B37 (1988) 1028.

* This calculation assumes a surface density of 1.50×10^{15} Pt atoms cm^{-2} for the (111) surface.

- 8 (a) A. Friedrich, B. Pettinger, D.M. Kolb, G. Lüpke, R. Steinhoff and G. Marowsky, *Chem. Phys. Lett.*, 163 (1989) 123; (b) G. Lüpke, G. Marowsky, R. Steinhoff, A. Friedrich, B. Pettinger and D.M. Kolb, *Phys. Rev.*, B41 (1990) 6913. (c) A. Friedrich, C. Shannon and B. Pettinger, *Surf. Sci.*, 251 (1991) 587.
- 9 (a) M.L. Lynch, and R.M. Corn, *J. Phys. Chem.*, 94 (1990) 4382. (b) M.L. Lynch, B.J. Barner and R.M. Corn, *J. Electroanal. Chem.*, 300 (1991) 447; (c) M.L. Lynch, B.J. Barner, M. Lantz and R.M. Corn, *J. Chim. Phys.*, 88 (1991) 1271.
- 10 A. Wieckowski, B.C. Schardt, S.D. Rosasco, J.L. Stickney and A.T. Hubbard, *Surf. Sci.*, 146 (1984) 115.
- 11 (a) D. Zurawski, L. Rice, M. Hourani and A. Wieckowski, *J. Electroanal. Chem.*, 230 (1987) 221; (b) M. Wasberg, L. Palaikis, S. Wallen, M. Kamrath and A. Wieckowski, *J. Electroanal. Chem.*, 256 (1988) 51.
- 12 (a) B.C. Schardt, S.L. Yau and F. Rinaldi, *Science*, 243 (1989) 1050; (b) S.L. Yau, C. M. Vitus and B.C. Schardt, *J. Am. Chem. Soc.* 112 (1990) 3677.
- 13 (a) J.L. Stickney, S.D. Rosasco, G.N. Salita and A.T. Hubbard, *Langmuir*, 1 (1985) 66; (b) F. Lu, F., G.N. Salita, H. Baltruschat and A.T. Hubbard, *J. Electroanal. Chem.*, 222 (1987) 305.
- 14 J.E. Sipe, D.J. Moss and H.M. van Driel, *Phys. Rev.*, B35 (1987) 1129.
- 15 P. Guyot-Sionnest, W. Chen, and Y.R. Shen, *Phys. Rev.*, B33 (1986) 8254.
- 16 M.L. Lynch, Ph.D. Thesis, University of Wisconsin–Madison, 1991.